Journal of proteome research

Article

pubs.acs.org/jpr

Metabotyping of Long-Lived Mice using ^{1}H NMR Spectroscopy

Anisha Wijeyesekera,[†,‡] Colin Selman,[‡,§] Richard H. Barton,[†] Elaine Holmes,[†] Jeremy K. Nicholson,*[,†] and Dominic J. Withers*[,∥]

[†]Biomolecular Medicine, Department of Surgery and Cancer, Faculty of Medicine, Imperial College London, South Kensington, London SW7 2AZ, United Kingdom

[§]Institute of Biological and Environmental Sciences, University of Aberdeen, Aberdeen, AB24 2TZ, United Kingdom

[∥]Metabolic Signaling Group, Medical Research Council Clinical Sciences Centre, Imperial College, London W12 0NN, United Kingdom

Supporting Information

ABSTRACT: Significant advances in understanding aging have been achieved through studying model organisms with extended healthy lifespans. Employing ^{1}H NMR spectroscopy, we characterized the plasma metabolic phenotype (metabotype) of three long-lived murine models: 30% dietary restricted (DR), insulin receptor substrate 1 null (*Irs1*$^{-/-}$), and Ames dwarf (Prop1$^{df/df}$). A panel of metabolic differences were generated for each model relative to their controls, and subsequently, the three long-lived models were compared to one another. Concentrations of mobile very low density lipoproteins, trimethylamine, and choline were significantly decreased in the plasma of all three models. Metabolites including glucose, choline, glycerophosphocholine, and various lipids were significantly reduced, while acetoacetate, D-3-hydroxybutyrate and trimethylamine-*N*-oxide levels were increased in DR compared to *ad libitum* fed controls. Plasma lipids and glycerophosphocholine were also decreased in *Irs1*$^{-/-}$ mice compared to controls, as were methionine and citrate. In contrast, high density lipoproteins and glycerophosphocholine were increased in Ames dwarf mice, as were methionine and citrate. Pairwise comparisons indicated that differences existed between the metabotypes of the different long-lived mice models. *Irs1*$^{-/-}$ mice, for example, had elevated glucose, acetate, acetone, and creatine but lower methionine relative to DR mice and Ames dwarfs. Our study identified several potential candidate biomarkers directionally altered across all three models that may be predictive of longevity but also identified differences in the metabolic signatures. This comparative approach suggests that the metabolic networks underlying lifespan extension may not be exactly the same for each model of longevity and is consistent with multifactorial control of the aging process.

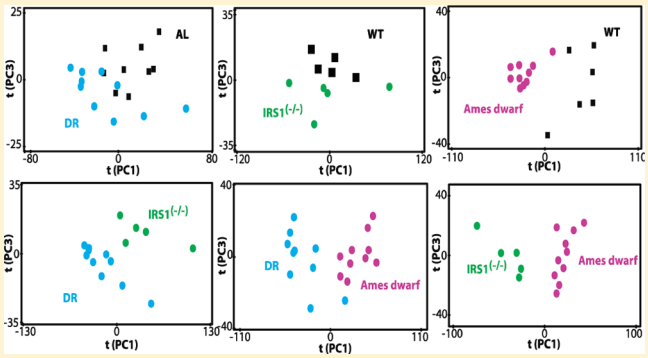

KEYWORDS: *metabolic phenotyping, metabotype, nuclear magnetic resonance, lifespan, aging, dietary restriction, Irs1, Ames dwarf*

INTRODUCTION

Life expectancy in humans is increasing rapidly,[1,2] with an estimated 30 years being added to average life expectancy in developed countries since 1900.[3] One unmistakable consequence of living longer is that the probability of developing diseases such as type 2 diabetes, osteoporosis, sarcopenia, and various cancers and dementias increases significantly with advancing age.[2,4−6] Therefore, a significant proportion of research into aging is engaged in identifying the mechanisms underlying the aging process. Patent obstacles exist in trying to understand what mechanisms underlie aging in humans over their entire lifespan. Therefore, short-lived model organisms such as yeast, the nematode worm *Caenorhabditis elegans*, the fruitfly *Drosophila melanogaster* and the mouse have proved invaluable to increasing our knowledge of the aging process.[5,7−9] Moreover, it is well established that significant commonality exists in the age-related pathologies suffered by both model organisms and humans.[5,10] Consequently, the challenge for researchers is to identify the mechanisms underlying healthy lifespan in model organisms to translate this knowledge into practical therapies for humans.

It has been established for several decades that dietary restriction (DR), a reduction in food intake without malnutrition, extends mean and maximum lifespan in a range of animals (for review, see ref 11). DR also improves age-related health in many organisms, including humans.[12,13] More recently, studies have demonstrated that aging can be modulated through genetic manipulation. For example, growth hormone (GH)/GH receptor-deficient dwarf mice,[14−17] various insulin/insulin-like growth factor (IGF) signaling (IIS) pathway mutant mice[18−22] and mammalian target of rapamycin (TOR) signaling mutant mice[23] are long-lived. In addition, several long-lived mice are also protected against age-related pathologies (for review, see ref 5). Pharmacological interventions acting on these pathways, including rapamycin[24,25] and metformin,[26,27] have also been shown to extend lifespan in mice.

Received: October 11, 2011
Published: January 6, 2012

   dx.doi.org/10.1021/pr2010154 | *J. Proteome Res.* 2012, 11, 2224−2235

Comparative transcriptional profiling has proved invaluable in demonstrating that significant transcriptional overlap and conservation exists between long-lived model organisms.[23,28−31] However, this approach cannot specifically inform what is happening at the post-transcriptional, post-translational or metabolic level.[32] Metabolic profiling has recently emerged as a platform to complement functional genomics in interrogating and profiling multiple biological processes in complex organisms. This technology can capture the effects of multiple interactions on the metabolic phenotypes (metabotypes) of individuals.[33−35] Metabolic profiling has been used widely in the search to identify disease biomarkers (e.g., see refs 36, 37). For example, elevated plasma levels of gut microbiota-derived metabolites of phosphatidylcholine, including choline and trimethylamine-*N*-oxide, identified using spectroscopic profiling were linked with cardiovascular disease pathogenesis in mice and humans.[38] Metabolic profiling has recently also been applied to aging-related research (for review, see ref 39). This technology has demonstrated that strain-specific differences in metabolite signatures in yeast were predictive of lifespan.[40] In addition, it has been shown that while long-lived dauer, IIS and translation-defective mutant *C. elegans* have distinct metabolite profiles relative to control animals, they share a common metabotype with one another.[32] However, a combinatorial approach in *C. elegans* using *daf-2*, *daf-16* and the di- and tripeptide transporter *pept-1* strains revealed mutant-specific metabolic signatures.[41] Significant age-related changes have also been identified in the rat brain[42] by spectroscopic profiling, and short-lived mice deficient for *ERCC1* were shown to differ significantly in plasma and urinary metabolites compared to control animals as they aged.[43] In addition, the enhanced insulin sensitivity of rhesus monkeys under DR was recently shown using a metabonomic approach to be linked to an increased flux in the pentose phosphate pathway.[44]

In the present study, we employed a systems approach to interrogate the biochemical and metabolic pathways, using ^{1}H NMR spectroscopy, in age-matched (16 weeks) male mice exposed to environmental (DR) or genetic (insulin receptor substrate 1 null, *Irs1*$^{-/-}$ null; Ames mice, *Prop1*$^{df/df}$) interventions known to extend healthy lifespan.[11,20,22,45] DR mice were exposed to 30% DR for 48 h, following a step-down DR protocol as previously described.[46] This level of DR has previously been shown to extend lifespan in mice (for review, see ref 11), and in addition, similar short-term periods of DR have been shown to capture many of the transcriptional changes induced following chronic DR.[46,47] The metabotypes of long-lived mice relative to their appropriate age-matched controls were characterized using an untargeted global profiling approach to more fully explore the metabolic signatures of long-lived mice. We then used pairwise comparisons to extract shared and unique features of the three long-lived mice metabotypes.

MATERIALS AND METHODS

Animal Handling

Male C57BL/6 mice for the DR experiment were purchased at 4 weeks of age from a commercial breeder (Harlan Laboratories, UK). The 30% DR cohort underwent a step-down feeding regime as previously described, that is, daily food intake was reduced to 90% of *ad libitum* (AL) fed mice at 14 wks of age, 80% at 15 wks, and maintained at 70% of *ad libitum* (AL) fed mice intake from 16 wks of age, that is, 30% DR relative to AL controls.[46,48] The DR food intake was adjusted according to the AL intake (per cage of 5 mice) measured over the preceding week. The generation and genotyping of *Irs1*$^{-/-}$ mice followed previously described protocols.[49] Ames dwarf mice were derived from a founder population purchased commercially (The Jackson Laboratory, Bar Harbor, ME). Mice were maintained in groups of 5 from weaning, and with the exception of the DR cohort, had *ad libitum* access to chow (2018 Teklad Global 18% Protein Rodent Diet, Harlan Teklad, U.K.). All animals were maintained as previously described,[20,22,46] under pathogen-free conditions within individually ventilated cages (Techniplast, Italy). All procedures followed local ethical and UK Home Office guidelines.

Plasma Collection

At 16 weeks of age and following an overnight fast, DR (exactly 48 h after the initiation of 30% DR), *Irs1*$^{-/-}$ and Ames mice plus their appropriate age-matched controls were culled. Blood plasma was collected as previously described[46] and stored at −80 °C pending analysis.

Sample Preparation

An aliquot of 200 μL of plasma from each mouse was pipetted into 5 mm outer diameter nuclear magnetic resonance (NMR) tubes. Samples were then diluted with 300 μL isotonic saline solution (0.9% w/v), 3 mM sodium azide in water and deuterium oxide (D_2O; 20% v/v), which acted as a field frequency lock for the NMR spectrometer.

^{1}H NMR Spectroscopic Analysis of Plasma Samples

^{1}H NMR spectra were recorded on a Bruker DRX-600 spectrometer (Bruker Biospin, Germany) operating at 600.13 MHz, with a probe temperature of 300 K. Spectra were acquired from all samples using the following standard one-dimensional standard pulse sequence with saturation of the water peak: Relaxation delay (RD) −90°-t_1-90°-t_m-90°-acquire free induction decay (FID): where 90° represents the applied 90°radio frequency (rf) pulse, t_1 is an interpulse delay set to a fixed interval of 3 μs, RD was 2 s and t_m (mixing time) was 150 ms. Water suppression was achieved through irradiation of the water signal during RD and t_m. Each plasma spectrum was acquired using 8 dummy scans, 128 scans, 32k time domain points with a spectral width of 12000 Hz. Standard ^{1}H NMR spectra yield information on both low and high molecular weight molecules. Broadness of resonances from relatively high concentration, high molecular weight molecules may obscure signals from lower intensity low molecular weight molecules. Therefore, two further ^{1}H NMR experiments were also performed on all plasma samples.

To attenuate broad signals from proteins and lipoproteins that may overlap signals from low molecular weight metabolites in plasma samples, 1D spin echo spectra were acquired using the Carr−Purcell−Meiboom−Gill sequence (CPMG[50,51]): RD-90°-(τ-180°-τ)n -acquire FID. Here, $t = 2n\tau$, where n = the number of spin echoes and t = CPMG delay time. A spin−spin relaxation delay of 64 ms was used for all samples and water suppression irradiation was applied during the relaxation delay (2 s) to achieve suppression of the water peak. All CPMG spectra were acquired using 8 dummy scans, 128 scans, 32k time domain points with a spectral width of 12000 Hz.

In order to further examine the effect of experimental manipulation on high molecular weight metabolites, we also analyzed high molecular weight molecules such as lipids and proteins using a diffusion-edited pulse sequence. Peak intensities were subsequently edited according to their molecular diffusion coefficients. Consequently, plasma lipid and protein moieties were less attenuated than those from small

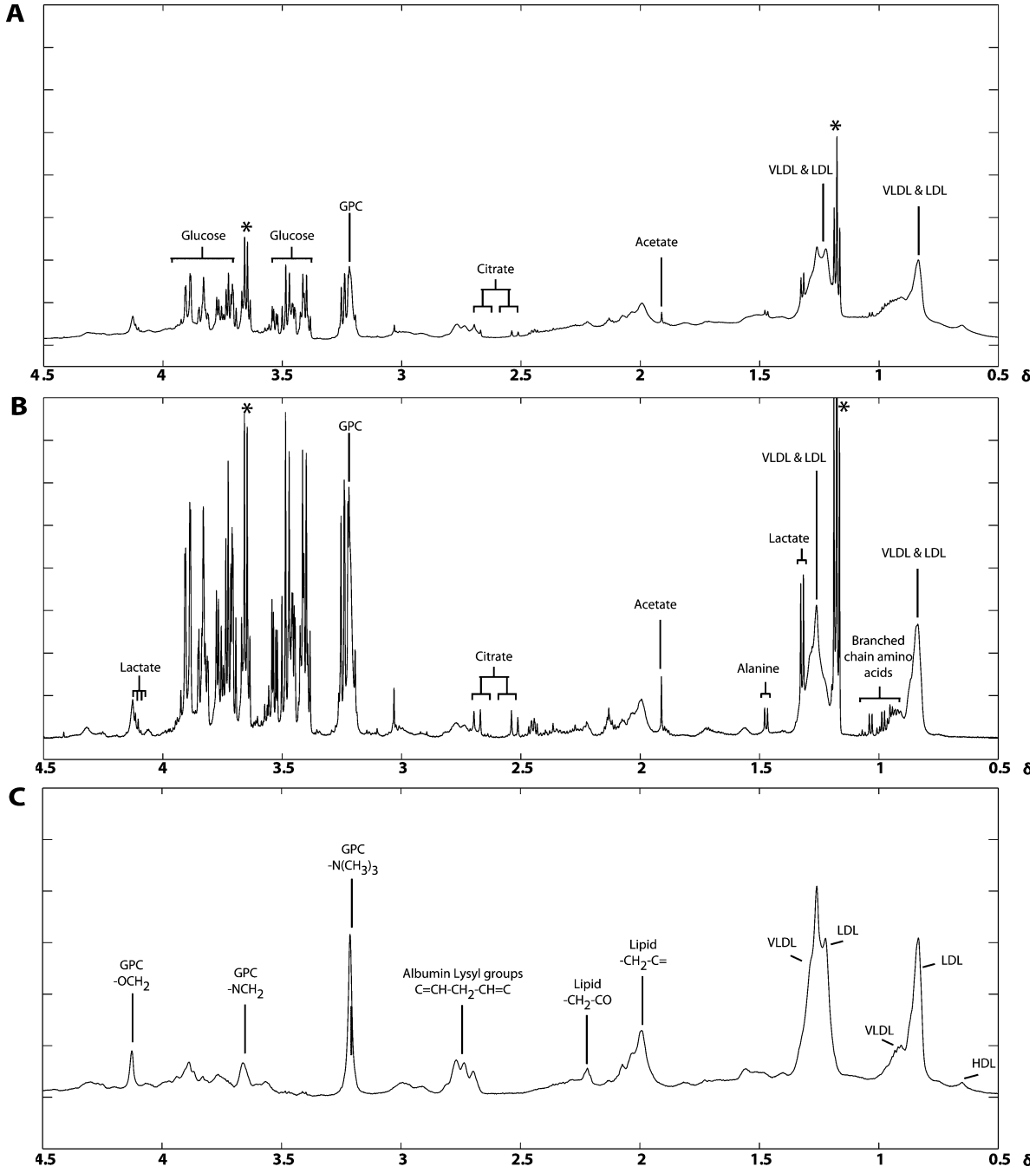

Figure 1. Aliphatic region (δ^1H 0.5−4.5) of exemplar ^{1}H NMR plasma spectra. Acquired using (A) standard 1D pulse sequence with presaturation suppression of the water peak, (B) the Carr−Purcell−Meiboom−Gill sequence to attenuate broad signals from proteins and lipoproteins that may overlap signals from low molecular weight metabolites, also using presaturation and (C) a diffusion edited pulse sequence to analyze high molecular weight molecules such as lipids and proteins. *Ethanol contaminant.

endogenous metabolites. 1D diffusion edited spectra were acquired using a bipolar-pair-longitudinal-eddy-current pulse sequence:[52,53] RD-90°-G_1-180°-G_1-90°-G_2-Δ-90°-G_1-180°-G_1-90°-G_2-t_e-90°-acquire FID. All spectra were acquired using 8 dummy scans, 256 scans, 16k time domain points with a spectral width of 12000 Hz.

Prior to Fourier transformation, FIDs were multiplied by an exponential function corresponding to a line broadening of 0.3 Hz for the standard 1D and CPMG experiments and 1.0 Hz for the diffusion edited experiment. Exemplar ^{1}H NMR spectra generated from the three NMR experiments are presented in Figure 1. All experiments were performed under randomized sample order conditions.

Multivariate Data Analysis

The 1D ^{1}H NMR plasma spectral data from the three long-lived mouse model experiments were manually phased, baseline corrected and referenced to the α-glucose anomeric doublet at δ 5.23, using XWIN-NMR software (Version 3.5, Bruker Biospin Ltd., UK). Spectral data were imported into Matlab (Version 7.6, The MathWorks Inc., Natick, MA), with spectral regions occupied by water (δ 4.45−5.15) and ethanol (δ 1.18 and 3.66) excluded (ethanol residues from antiseptic swabbing

dx.doi.org/10.1021/pr2010154 | J. Proteome Res. 2012, 11, 2224−2235

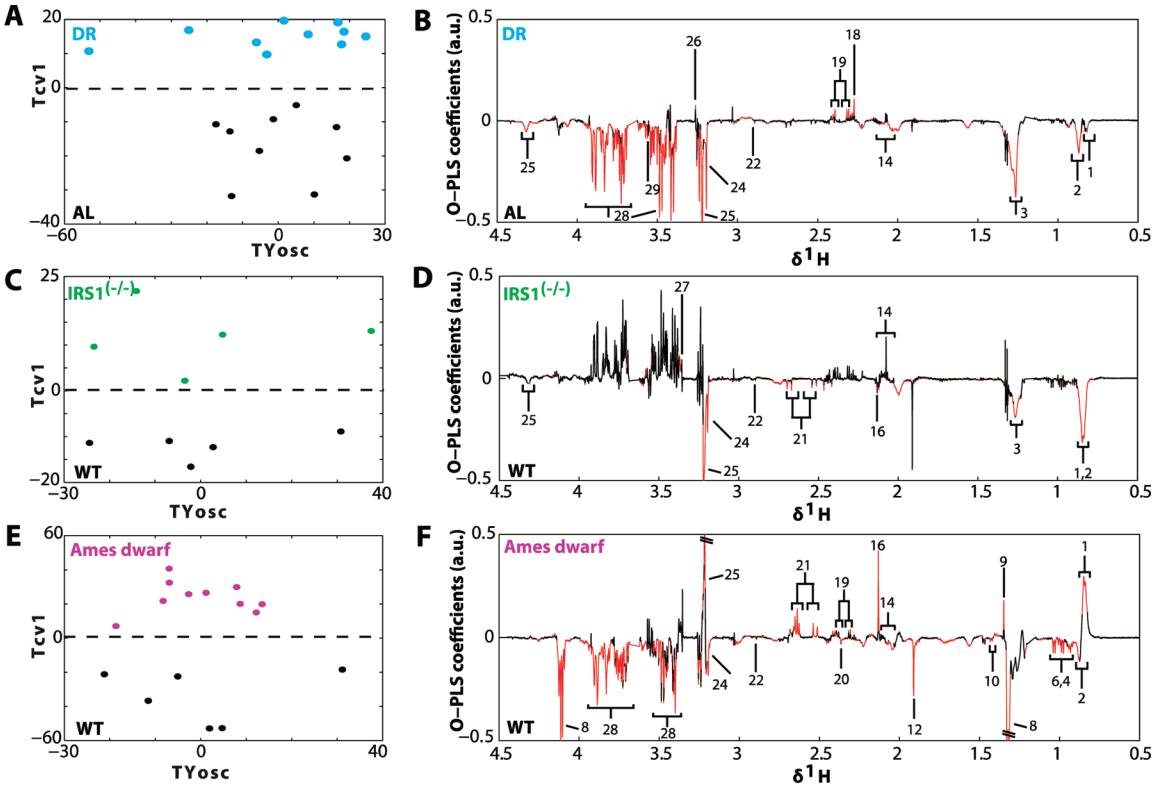

Figure 2. Results of pairwise supervised multivariate modeling performed on CPMG plasma spectroscopic data for each long-lived model vs respective control: O-PLS-DA cross validated scores scatter plot showing the clustering of samples according to metabotype; corresponding O-PLS-DA loadings coefficients plot back-projected with *p*-values, showing the plasma metabolites discriminating between metabotype (models computed using 1 predictive component, 2 orthogonal components in X, 0 orthogonal components in Y, 7-fold cross-validation). (A) O-PLS-DA cross-validated scores of DR and AL mice; (B) O-PLS-DA loadings of DR and AL mice ($R^2Y = 0.91$, $Q^2Y = 0.85$). (C) O-PLS-DA cross-validated scores of *Irs1*$^{-/-}$ and WT control mice; (D) O-PLS-DA loadings of *Irs1*$^{-/-}$ and WT control mice ($R^2Y = 0.93$, $Q^2Y = 0.86$). (E) O-PLS-DA cross-validated scores of Ames dwarf and WT control mice; (F) O-PLS-DA loadings of Ames dwarf and WT control mice ($R^2Y = 0.95$, $Q^2Y = 0.84$). Refer to Table 1 for assignments of discriminatory metabolites.

contaminated some plasma samples during collection). Plasma spectral data points were then aligned[54] and subsequently normalized with probabilistic quotient normalization[55] to reduce the effects of differential dilution or concentration on the data analysis, using proprietary Matlab scripts. The resulting data matrices were interpreted using principal component analysis (PCA) to discern the presence of inherent similarities in the spectral profiles[56] and to identify outliers. Unsupervised multivariate analysis was performed using the SIMCA-P+ (Version 12.5, Umetrics AB, Sweden) software package using mean centered data with no further scaling. Further supervised pattern recognition was then carried out on the normalized plasma spectra using mean centered data, to characterize the differences in metabotype in each long-lived aging model compared with their age-matched wild type control. This was achieved using orthogonal projections to latent structure discriminant analysis (O-PLS-DA), a method based on projections to latent structure (PLS) analysis.[57] An in-built orthogonal filter, coded in-house in Matlab,[58] was used to perform data analysis without the requirement of any reduction of the original ^{1}H NMR spectral resolution. Pairwise O-PLS-DA models were constructed to systematically identify metabolites contributing to the differences between the long-lived model, using the NMR spectroscopic data as the X variables, and each experimental modification as the Y variable, describing class ownership (long-lived model versus control) of the animals. The statistical significance and validity of the O-PLS-DA results were calculated using a permutation test (number of permutations = 10000).[59] Each pairwise O-PLS-DA model was interpreted by means of statistically significant ($p \leq 0.05$) O-PLS coefficients. Resonance assignments were made with reference to existing literature[60] and statistical total correlation spectroscopy (STOCSY), a spectroscopic correlation method coded in Matlab.[61]

RESULTS

Exemplar spectra acquired using standard 1D (A), CPMG (B) and diffusion edited (C) ^{1}H NMR experiments are shown in Figure 1. Typical median ^{1}H CPMG NMR plasma spectra obtained from each mouse strain or treatment pair (long-lived mouse model and control) are shown in Supplementary Figure S1, Supporting Information.

To characterize the differences in the metabolic profile between each pair, pairwise multivariate models were calculated for each long-lived mouse mutant. The PCA scores plot from each long-lived model showed clear differentiation of plasma profiles from corresponding age-matched controls (see Supplementary Figure S2, Supporting Information). Since the class information is not used in the PCA model, these data demonstrate inherent metabolic differences in circulating plasma metabolites between long-lived and control mice. To identify the plasma metabolites responsible for the differentiation between each pair, a supervised O-PLS-DA model was then obtained for each individual model of longevity. O-PLS-DA modeling indicated separation of each long-lived model from its appropriate control in the first principal component, shown in Figures 2A–F for DR, *Irs1*$^{-/-}$ and Ames dwarf mice, respectively.

dx.doi.org/10.1021/pr2010154 | *J. Proteome Res.* 2012, 11, 2224–2235

Table 1. O-PLS-DA Pairwise Comparisons of Long-Lived Mouse Models[a]

		DR vs AL (R^2Y = 0.91, Q^2Y = 0.85)[b]	*Irs1*$^{-/-}$ vs WT (R^2Y = 0.93, Q^2Y = 0.86)[b]	Ames vs WT (R^2Y = 0.95, Q^2Y = 0.84)[b]	DR vs *Irs1*$^{-/-}$ (R^2Y = 0.99, Q^2Y = 0.98)[b]	DR vs Ames (R^2Y = 0.95, Q^2Y = 0.90)[b]	*Irs1*$^{-/-}$ vs Ames (R^2Y = 0.99, Q^2Y = 0.86)[b]
1	0.84 (m) HDL	–	–	+		–	–
2	0.88 (m) Lipid (mainly VLDL)	–	–	–			
3	1.26 (m) Lipid (mainly LDL)	–	–			–	–
4	0.93 (t), 1.00 (d) Isoleucine			–		+	+
5	0.96 (t) Leucine						–
6	0.98 (d), 1.03 (d) Valine			–		+	+
7	1.06 (d) Unassigned Metabolite (U1)				–	–	+
8	1.32 (d), 4.11 (q) Lactate			–		–	
9	1.35 (s) 2-hydroxyisobutyrate			+		–	–
10	1.42 (d) Unassigned Metabolite (U2)			–	–	–	
11	1.47 (d) Alanine				–	–	
12	1.91 (s) Acetate			–	–		+
13	2.03 (s) *N*-acetyl glycoprotein (NAG) associated resonances				–	–	
14	2.06 (s) *N*-acetyl glycoprotein (NAG) associated resonances	–	+	+	–	+	+
15	2.08 (s), 2.10 (s) *N*-acetyl glycoprotein (NAG) associated resonances				–	–	+
16	2.13 (s), 2.64 (t) Methionine		–	+	+	–	–
17	2.22 (s) Acetone				–	+	+
18	2.27 (s) Acetoacetate	+				+	+
19	2.31 (d), 2.38 (d) D-3-hydroxybutyrate	+		+			+
20	2.36 (s) Pyruvate			–	–		+
21	2.52 (d), (d) 2.68 Citrate		–	+	+	+	+
22	2.89 (s) Trimethylamine	–	–	–			
23	3.03 (s), 3.93 (s) Creatine				–	–	+
24	3.19 (s) Choline	–	–	–		–	–
25	3.22 (s), 4.30 (m) Glycerophosphocholine	–	–	+	–	–	–
26	3.26 (s) Trimethylamine-*N*-Oxide (TMAO)	+			+	+	
27	3.35 (s) *Scyllo*-inositol		+		–	–	–
28	(t) 3.40 – (dd) 3.90 α- and β-glucose	–		–	–	+	+
29	3.56 (s) Glycine	–				–	

[a]Metabolites statistically ($P < 0.05$) different in peak intensity are listed by order of chemical shift. + indicates an increase in plasma concentration and – denotes a decrease in plasma concentration in the first named mice relative to the second named mice. DR, dietary restriction; AL, *ad libitum* control, WT, wild type control. [b]Goodness of fit (R^2Y) and goodness of prediction (Q^2Y) statistics are shown for each pairwise model.

The metabotype of DR mice exhibited a set of resonances that differed significantly from AL controls in the levels of several spectral resonances (Figure 2A–B). The plasma levels of acetoacetate, D-3-hydroxybutyrate and trimethylamine-*N*-oxide (TMAO) were all elevated (Table 1). Considerably more plasma metabolites were significantly reduced in concentration DR mice relative to AL mice; residual signals from mobile high density lipoprotein (HDL), low density lipoprotein (LDL), very low density lipoprotein (VLDL), *N*-acetyl glycoprotein fragments, glucose, glycine, choline, glycerophosphocholine and trimethylamine (TMA). In common with DR mice, *Irs1*$^{-/-}$ mice had lower mobile plasma HDL, LDL, VLDL, TMA, choline, and glycerophosphocholine (Figure 2C–D; Table 1). However, *Irs1*$^{-/-}$ mice also had significantly lower plasma methionine and citrate relative to WT controls, and increased *N*-acetyl glycoprotein resonances and *scyllo*-inositol. Ames dwarfs, unlike DR and *Irs1*$^{-/-}$ mice, had elevated HDL and glycerophosphocholine relative to controls (Figure 2E–F; Table 1). In contrast to *Irs1*$^{-/-}$ mice, Ames mice had significantly higher plasma methionine, and citrate relative to controls. In common with DR mice, Ames mice had significantly decreased glucose levels and significantly elevated D-3-hydroxybutyrate compared with WT controls. In terms of metabolic commonality, only three sets of resonances; triglycerides (mainly the more mobile VLDL), TMA and choline, were significantly altered (decreased) across all three long-lived mice (Table 1).

In order to compare metabolic profiles across long-lived mice, we derived pairwise (O-PLS-DA) models comparing DR mice to *Irs1*$^{-/-}$ mice (Figure 3A–B), DR mice to Ames dwarf mice (Figure 3C–D) and *Irs1*$^{-/-}$ mice to Ames dwarf mice (Figure 3E–F; results from unsupervised PCA are shown in Supplementary Figure S3, Supporting Information). This analysis showed significant metabolic differences in circulating plasma of long-lived mice (Table 1). DR mice had significantly lower plasma levels of alanine, acetate, creatine, glycerophos-

dx.doi.org/10.1021/pr2010154 | J. Proteome Res. 2012, 11, 2224–2235

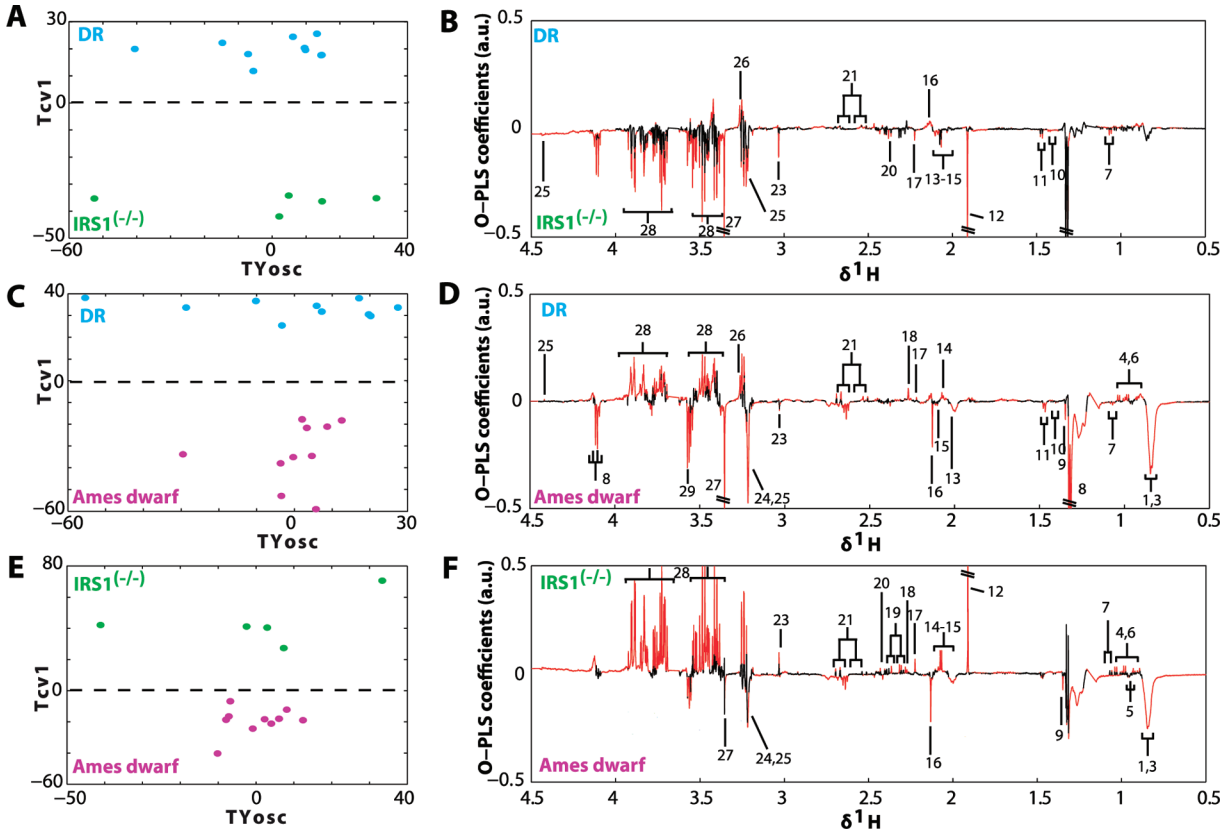

Figure 3. Results of pairwise supervised multivariate modeling performed on CPMG plasma spectroscopic data for each long-lived model vs long-lived model (models computed using 1 predictive component, 2 orthogonal components in X, 0 orthogonal components in Y, 7-fold cross-validation). (A) O-PLS-DA cross-validated scores of DR and *Irs1*$^{-/-}$ mice; (B) O-PLS-DA loadings of DR and *Irs1*$^{-/-}$ mice ($R^2Y = 0.99$, $Q^2Y = 0.98$). (C) O-PLS-DA cross-validated scores of DR and Ames dwarf mice; (D) O-PLS-DA loadings of DR and Ames dwarf mice ($R^2Y = 0.95$, $Q^2Y = 0.90$). (E) O-PLS-DA cross-validated scores of *Irs1*$^{-/-}$ and Ames dwarf mice; (F) O-PLS-DA loadings of *Irs1*$^{-/-}$ and Ames dwarf ($R^2Y = 0.99$, $Q^2Y = 0.86$). Refer to Table 1 for assignments of discriminatory metabolites.

phocholine and *scyllo*-inositol compared to the other long-lived mice, but elevated citrate and TMAO. Plasma levels of acetate, acetone, creatine and glucose were elevated, but methionine was significantly reduced in *Irs1*$^{-/-}$ mice compared to DR and Ames mice. Ames mice were characterized by elevated mobile lipoproteins, 2-hydroxyisobutyrate, methionine, choline, glycerophosphocholine and *scyllo*-inositol compared to DR and *Irs1*$^{-/-}$ mice. However, Ames mice also had significantly lower isoleucine, valine, acetone, acetoacetate, citrate and glucose levels compared to the other 2 models (Table 1). Plasma lipoprotein differences appeared to dominate the metabolic signatures of the three mouse models even in the CPMG spectral data used for multivariate modeling, which only contained attenuated signals from the higher molecular weight species. Therefore, in addition, we analyzed diffusion edited spectral data acquired from all plasma samples, to specifically assess the differences in high molecular weight metabolites (Figures 4 and 5). These results were mostly in agreement with the differences in lipid profiles observed with CPMG spectral data (direction); however, the significance of these lipoprotein differences in some cases did not match what we observed in CPMG data. The fact that the significance of the lipoprotein contribution to the differential profile was greater in the CPMG than in the diffusion edited spectra would indicate that the differences are mainly due to the more mobile lipid species since the diffusion edited pulse sequence selects against the more mobile species.

DISCUSSION

Systematic differences were seen between all three long-lived mouse models and their respective controls, as evidenced from the ^{1}H NMR plasma spectroscopic profiles and subsequent multivariate modeling of the spectral data. However, a consequent three-way comparison indicated that while some overlap existed in the metabolic signatures of these mice, clear differences existed between metabotypes of these long-lived models. These findings are somewhat in contrast to the transcriptomic commonality observed both within and between long-lived species.[23,28−31,62] Commonality in the metabolic signature across different long-lived *C. elegans* has been reported,[32] although a second study, again using ^{1}H NMR, reported a clear separation in the metabolic profiles across different long-lived worm mutants.[41]

Plasma spectroscopic data from DR and *ad libitum* (AL) controls indicated a metabolic switch toward gluconeogenesis and energy conservation in DR mice, as previously reported (e.g., ref 46). The level of plasma glucose was significantly reduced by DR, whereas acetoacetate and D-3-hydroxybutyrate were increased, consistent with a greater requirement for ketone body utilization. As with DR mice, *Irs1*$^{-/-}$ mice, which like DR mice remain lean throughout their life,[20] had a significantly reduced plasma lipid profile. For this comparative study we focused on analysis of CPMG spectral data rather than standard 1D ^{1}H NMR spectroscopic data, in order to characterize the differences in signals from low molecular

dx.doi.org/10.1021/pr2010154 | J. Proteome Res. 2012, 11, 2224−2235

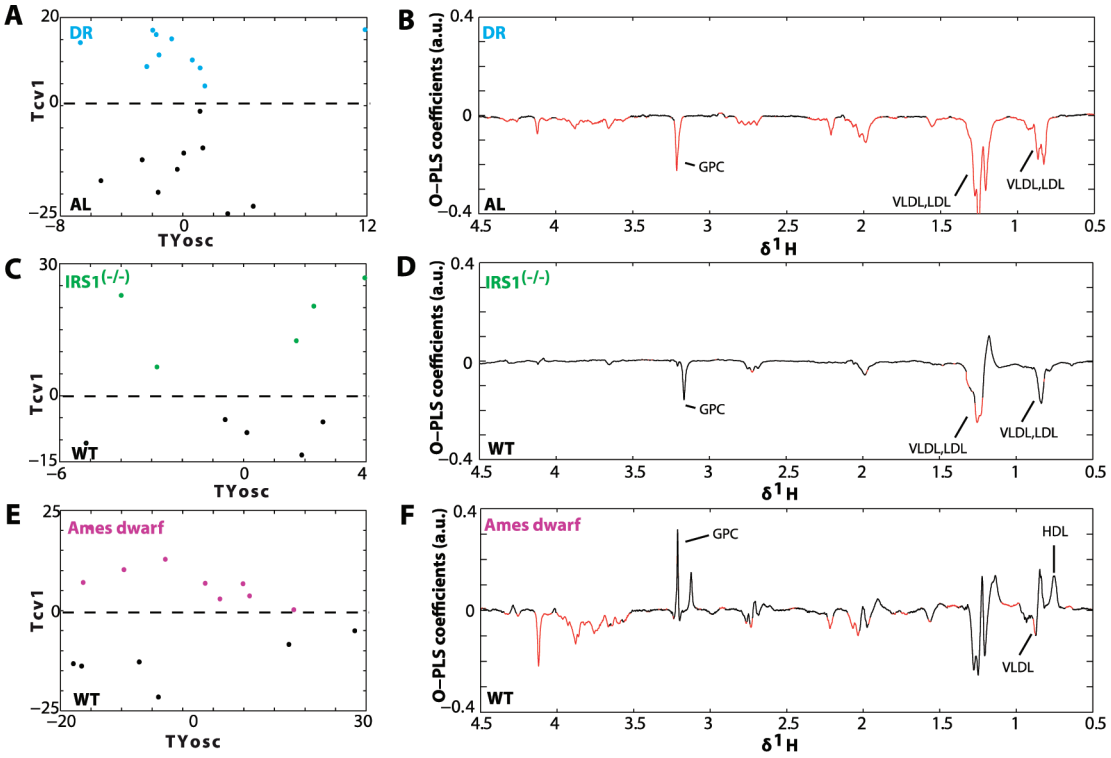

Figure 4. Results of pairwise supervised multivariate modeling performed on Diffusion Edited plasma spectroscopic data for each long-lived model vs respective control. (A) O-PLS-DA cross-validated scores of DR and AL mice; (B) O-PLS-DA loadings of DR and AL mice (R^2 = 0.88, Q^2 = 0.85). (C) O-PLS-DA cross-validated scores of *Irs1*$^{-/-}$ and WT control mice; (D) O-PLS-DA loadings of *Irs1*$^{-/-}$ and WT control mice (R^2 = 0.86, Q^2 = −0.51). (E) O-PLS-DA cross-validated scores of Ames dwarf and WT control mice; (F) O-PLS-DA loadings of Ames dwarf and WT control mice (R^2 = 0.87, Q^2 = 0.75). Lipoproteins discriminating between models are labeled in Table 1.

weight metabolites that may be overlapped by broad signals from proteins and lipoproteins. Thus, the differences in plasma lipid profile that we observed between mice models can be attributed to residual signals from mobile lipoproteins. This is also evidenced by the apparent disproportional lipid methyl and methylene signals in the CPMG spectral data (Figure 2D and Figure 3D), which is caused by differential transverse relaxation (T2) times from mobile lipid species. For this reason we conducted analysis of diffusion edited spectral data acquired from the same plasma samples, which revealed the same differences in lipid profile as the CPMG spectral data (Figures 4 and 5), confirming the differences between lipid species between the long-lived mice models and matched controls. Consistent with our findings, differences in plasma lipid profiles were also reported in a caloric restriction study in dogs,[63] supporting a common characteristic of long-lived models. Plasma glucose levels were elevated in *Irs1*$^{-/-}$ mice, but ketone bodies were unaltered, in agreement with the well reported metabolic phenotype of these mice.[20,64,65] The tricarboxylic acid (TCA) intermediate citrate, which may also play a role in amino acid and fatty acid metabolism,[66] was decreased in *Irs1*$^{-/-}$ mice, but elevated in Ames mice, relative to controls. Elevated plasma citrate levels inhibit phosphofructokinase, a regulatory enzyme in glycolysis, and glycolytic inhibitors such as 2-deoxyglucose have been put forward as viable DR mimetics.[67] While mitochondrial function has not been examined in *Irs1*$^{-/-}$ mice, it is well established that Ames mice have enhanced mitochondrial function and efficiency compared to controls.[68] *Scyllo*-inositol, a stereoisomer of the carbohydrate inositol, was also significantly elevated in the plasma of *Irs1*$^{-/-}$ mice. Interestingly, supplementation with *scyllo*-inositol has been shown to attenuate disease pathology and cognitive deficits in mouse models of Alzheimer disease.[69]

The essential amino acid methionine was also significantly reduced in *Irs1*$^{-/-}$ mice relative to controls. Methionine restriction has previously been reported to increase lifespan in rodents,[70,71] to reduce serum insulin, IGF-1 and glucose levels,[70,72] increase stress resistance and delay several age-related pathologies.[70] However, in contrast, Ames mice had increased plasma methionine relative to controls, and an enhanced methionine flux to transsulfuration has been associated with the improved oxidative stress resistance in Ames mice.[73,74] Although the exact causative role of oxidative stress in lifespan determination is ambiguous,[75,76] it will be interesting to determine whether *Irs1*$^{-/-}$ mice have an altered stress response to oxidative insult. The branched amino acids isoleucine and valine were also decreased in Ames mice, perhaps suggestive of reduced muscle turnover. As with DR mice, the ketone body D-3-hydroxybutyrate was increased in Ames mice, while glucose levels were significantly decreased as previously reported.[77] Mobile plasma VLDL was also reduced in Ames mice, whereas HDL was increased relative to controls. Plasma HDL was decreased in DR and *Irs1*$^{-/-}$ mice, and significantly elevated in Ames mice relative to the other two models. HDLs have a key role in cardioprotection,[78] and the lower HDL in DR mice may be specific to the early life DR regime applied here, as more chronic DR increases plasma HDLs.[78,79] 2-Hydroxyisobutyrate (2-HIBA), which is produced following degradation of dietary proteins by gut microbes,[80] was increased in Ames dwarfs relative to WT controls. Interestingly, 2-HIBA can be metabolized to D-3-hydroxybutyrate (also elevated in Ames dwarfs), via a cobalamin-dependent

dx.doi.org/10.1021/pr2010154 | *J. Proteome Res.* 2012, 11, 2224−2235

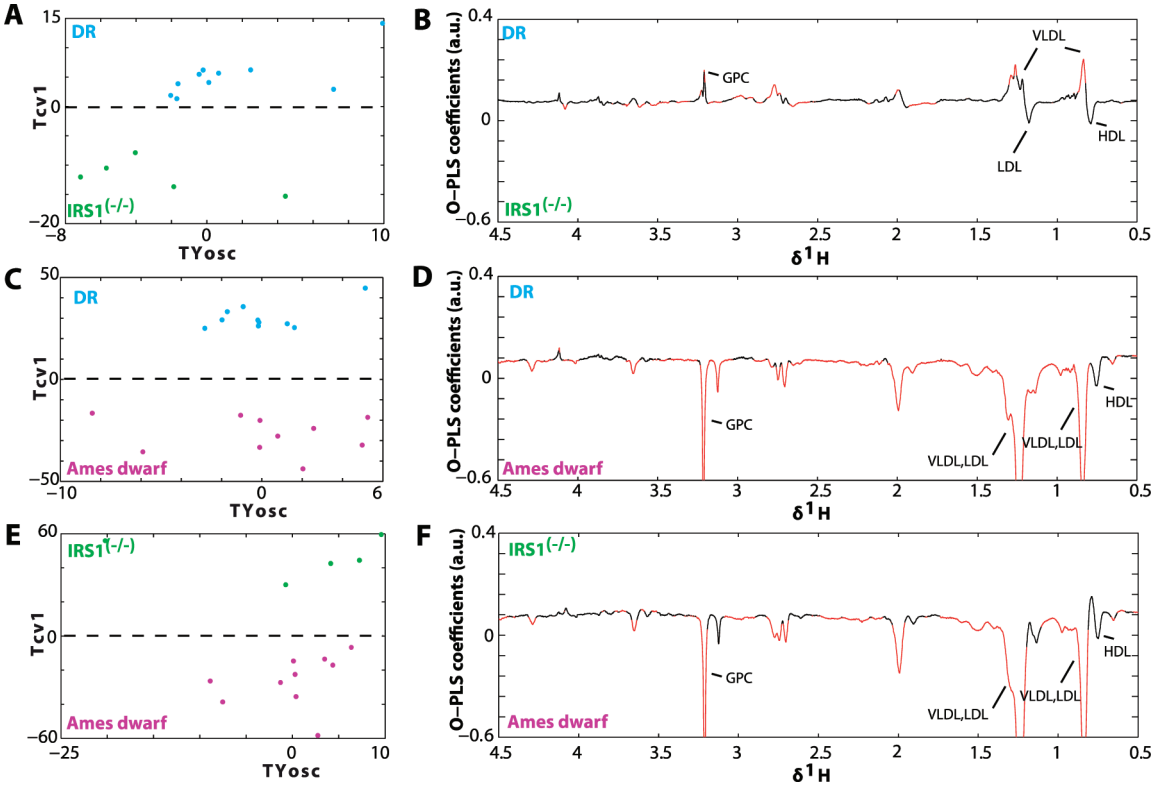

Figure 5. Results of pairwise supervised multivariate modeling performed on Diffusion Edited plasma spectroscopic data for each long-lived model vs long-lived model. (A) O-PLS-DA cross-validated scores of DR and *Irs1*$^{-/-}$ mice; (B) O-PLS-DA loadings of DR and *Irs1*$^{-/-}$ mice (R^2 = 0.89, Q^2 = 0.42). (C) O-PLS-DA cross-validated scores of DR and Ames dwarf mice; (D) O-PLS-DA loadings of DR and Ames dwarf mice (R^2 = 0.96, Q^2 = 0.89). (E) O-PLS-DA cross-validated scores of *Irs1*$^{-/-}$ and Ames dwarf mice; (F) O-PLS-DA loadings of *Irs1*$^{-/-}$ and Ames dwarf (R^2 = 0.93, Q^2 = 0.86). Lipoproteins discriminating between models are labeled in Table 1.

mutase reaction.[81] As changes in gut microbiota have been linked to age-related disease,[97,98] it would be fascinating to use this approach to determine whether long-lived mice have some commonality in their gut microbiota. A recent study by Wang et al.[38] showed that plasma TMAO levels in germ free mice were dependent upon the microbiota. To further probe the role of the gut microbiota it would be expedient to conduct metabolic profiling analysis on urine, which is known to report on several classes of microbial metabolites. Other strategies to investigate the role of the microbiota in long-lived mice models would include high-throughput sequencing of the fecal microbiome or metabolic profiling of fecal water.

In terms of metabolic commonality, three metabolites choline, TMA and mobile lipids (mainly VLDL) were significantly altered (decreased) in all three long-lived mice relative to their appropriate controls. The essential nutrient choline has a wide range of cellular effects (for review, see refs 82, 83). It acts as a lipotrophic agent, and so low choline levels may be important in long-lived mice that are already significantly leaner than controls.[20,48,84] Choline is also involved in synthesizing the phospholipids, sphingomyelin and phosphatidylcholine, which are precursors for diacylglycerols and ceramides. Both diacylglycerols and ceramides have been suggested as key mediators of insulin resistance and lipotoxicity.[85] Ceramides can also induce inflammation and block both insulin action and glucose uptake through inhibiting *Akt*.[85] Therefore, low plasma levels of choline may result in low levels of these secondary metabolites, which appear to have negative consequences for several parameters associated with health. Interestingly, mice null for phosphatidylethanolamine *N*-methyltransferase, a key enzyme in the synthesis of choline, are resistant to the body mass and insulin resistant effects of diet induced obesity.[86] Choline can also act as a methyl group source and plays a key role in acetylcholine synthesis.[82,83] Thus an alternative explanation of the lower plasma choline levels of long-lived mice may be enhanced neurotransmitter biosynthesis, with all three models demonstrating preserved neurological function during aging.[20,87−89] Recently elevated plasma levels of both choline and TMA were shown to both be risk factors for cardiovascular disease in humans.[38] This same study demonstrated that dietary supplementation of phosphidylcholine metabolites, including choline, induced atherosclerosis in mice.[38] The presence of cardiovascular disease, and its role in mortality, is assumed to negligible in long-lived mouse models. However, both Ames dwarfs[90] and DR mice[91] have reduced cardiac cell size and decreased extracellular collagen compared to control animals. DR also decreases atherosclerosis significantly in apolipoprotein E-deficient mice.[92]

In our comparison of metabolite profiles between long-lived mice, it was apparent that several metabolites differed on a relative scale between the long-lived mice. One caveat of this comparative approach is that genetic strain may play a confounding role, with DR and *Irs1*$^{-/-}$ mice maintained on a C57BL/6 background and Ames mice maintained on a mixed genetic background. Nonetheless, elevated plasma glucose levels were observed in *Irs1*$^{-/-}$ mice compared to DR and Ames mice, perhaps unsurprisingly. This is completely in accord with their well-described metabolic phenotype.[20,65] Ames mice had significantly lower plasma glucose levels than mice under 30% DR. It has previously been reported that DR

dx.doi.org/10.1021/pr2010154 | *J. Proteome Res.* 2012, 11, 2224−2235

does not additionally reduce plasma glucose levels in Ames dwarf mice.[93] Plasma methionine levels were higher in DR and Ames mice compared to *Irs1*$^{-/-}$ mice and highest in Ames dwarfs. As discussed above, altered methionine metabolism is implicated in the enhanced oxidative stress response in these animals.[73] It is possible that this altered metabolism is GH-dependent, as GH treatment in Ames mice abolished this effect[94] and *Irs1*$^{-/-}$ mice, despite being dwarf, have normal somatotrophic function.[20] Our comparative approach also suggests that DR and *Irs1*$^{-/-}$ mice may be more dependent on utilizing ketone bodies as an energy source than Ames mice. Creatine, which acts to shuttle high energy phosphate between mitochondria and the sites of utilization, for example, myofibers,[95] was lowest in DR mice, and lower in Ames dwarfs than *Irs1*$^{-/-}$ mice. Urinary creatine levels were elevated in two rat models (Zucker obese and Goto-kakizaki) of type 2 diabetes.[96] Plasma creatine is a marker of lean muscle mass, and higher levels may also indicate increased physical activity levels.[80] However, it is currently unknown whether relative differences exist in lean muscle mass and locomotor activity between long-lived mice strains. As mentioned earlier, glycolytic inhibition has been suggested as a means to develop DR mimetics.[67] Interestingly, citrate was significantly elevated in DR mice compared to the other two mouse models and also elevated in *Irs1*$^{-/-}$ mice compared to Ames dwarfs.

CONCLUSIONS

This study is the first to use metabotyping to compare plasma metabolite levels both within and between long-lived mouse models. We show that commonality exists across long-lived DR, *Irs1*$^{-/-}$ and Ames mice, particularly in metabolites associated with phosphatidylcholine metabolism. This commonality may suggest that these metabolites could be used as appropriate biomarkers for longevity and second that there is some conservation in the metabolic processes underlying increased healthy lifespan, as seen in *C. elegans*.[32] However, what is also evident from this novel approach is that distinct metabolic signatures are associated with specific long-lived mice, as in *C. elegans*.[41] We suggest that metabonomic technology can provide further insights into the "functional genotype"[41] of an individual organism and will allow repeated measures of the same individual across its lifespan. In addition, this technology will enable researchers to examine complex metabolic pathways occurring in a tissue-specific manner of long-lived mice.

ASSOCIATED CONTENT

Supporting Information

Supplementary Figures S1–S3. This material is available free of charge via the Internet at http://pubs.acs.org.

AUTHOR INFORMATION

Corresponding Author

*Dominic J. Withers, Metabolic Signaling Group, Medical Research Council Clinical Sciences Centre, Imperial College, London W12 0NN, U.K. Phone: +44 (0) 208 383 3014. Fax: +44 (0) 208 383 8303. E-mail: d.withers@imperial.ac.uk. Jeremy K. Nicholson, Biomolecular Medicine, Department of Surgery and Cancer, Faculty of Medicine, Imperial College London, South Kensington, London SW7 2AZ, U.K. Tel: +44 (0) 207 594 3195. Fax: +44 (0) 207 594 3226. E-mail: j.nicholson@imperial.ac.uk.

Author Contributions

‡These authors contributed equally to this work.

ACKNOWLEDGMENTS

We are grateful to Steve Lingard for his invaluable help and input during these studies. We thank the Biological Services Unit staff, at University College London, and Imperial College, London U.K. for animal care.

REFERENCES

(1) Vaupel, J. W. Biodemography of human ageing. *Nature* **2010**, *464* (7288), 536–42.
(2) Partridge, L.; Thornton, J.; Bates, G. The new science of ageing. *Philos. Trans. R. Soc. Lond., B: Biol. Sci.* **2011**, *366* (1561), 6–8.
(3) Christensen, K.; Doblhammer, G.; Rau, R.; Vaupel, J. W. Ageing populations: the challenges ahead. *Lancet* **2009**, *374* (9696), 1196–208.
(4) Partridge, L. The new biology of ageing. *Philos. Trans. R. Soc. Lond., B: Biol. Sci.* **2010**, *365* (1537), 147–54.
(5) Selman, C.; Withers, D. J. Mammalian models of extended healthy lifespan. *Philos. Trans. R. Soc. Lond., B: Biol. Sci.* **2011**, *366* (1561), 99–107.
(6) Fontana, L.; Partridge, L.; Longo, V. D. Extending healthy life span--from yeast to humans. *Science* **2010**, *328* (5976), 321–6.
(7) Piper, M. D.; Selman, C.; McElwee, J. J.; Partridge, L. Separating cause from effect: how does insulin/IGF signalling control lifespan in worms, flies and mice? *J. Intern. Med.* **2008**, *263* (2), 179–91.
(8) Partridge, L.; Alic, N.; Bjedov, I.; Piper, M. D. Ageing in Drosophila: The role of the insulin/Igf and TOR signalling network. *Exp. Gerontol.* **2011**, *46* (5), 376–81.
(9) Kenyon, C. The first long-lived mutants: discovery of the insulin/IGF-1 pathway for ageing. *Philos. Trans. R. Soc. Lond., B: Biol. Sci.* **2011**, *366* (1561), 9–16.
(10) Vijg, J.; Campisi, J. Puzzles, promises and a cure for ageing. *Nature* **2008**, *454* (7208), 1065–71.
(11) Weindruch, R.; Walford, R. L. *The Retardation of Aging and Disease by Dietary Restriction*; Charles C. Thomas: Springfield, IL, 1988.
(12) Fontana, L.; Meyer, T. E.; Klein, S.; Holloszy, J. O. Long-term calorie restriction is highly effective in reducing the risk for atherosclerosis in humans. *Proc. Natl. Acad. Sci. U.S.A.* **2004**, *101* (17), 6659–63.
(13) Fontana, L.; Villareal, D. T.; Weiss, E. P.; Racette, S. B.; Steger-May, K.; Klein, S.; Holloszy, J. O. Calorie restriction or exercise: effects on coronary heart disease risk factors. A randomized, controlled trial. *Am. J. Physiol. Endocrinol. Metab.* **2007**, *293* (1), E197–202.
(14) Bartke, A. Single-gene mutations and healthy ageing in mammals. *Philos. Trans. R. Soc. Lond., B: Biol. Sci.* **2011**, *366* (1561), 28–34.
(15) Bartke, A.; Brown-Borg, H. Life extension in the dwarf mouse. *Curr. Top. Dev. Biol.* **2004**, *63*, 189–225.
(16) Bonkowski, M. S.; Rocha, J. S.; Masternak, M. M.; Al Regaiey, K. A.; Bartke, A. Targeted disruption of growth hormone receptor interferes with the beneficial actions of calorie restriction. *Proc. Natl. Acad. Sci. U.S.A.* **2006**, *103* (20), 7901–5.
(17) Coschigano, K. T.; Holland, A. N.; Riders, M. E.; List, E. O.; Flyvbjerg, A.; Kopchick, J. J. Deletion, but not antagonism, of the mouse growth hormone receptor results in severely decreased body weights, insulin, and insulin-like growth factor I levels and increased life span. *Endocrinology* **2003**, *144* (9), 3799–810.
(18) Bluher, M.; Kahn, B. B.; Kahn, C. R. Extended longevity in mice lacking the insulin receptor in adipose tissue. *Science* **2003**, *299* (5606), 572–4.
(19) Kappeler, L.; De Magalhaes Filho, C. M.; Dupont, J.; Leneuve, P.; Cervera, P.; Perin, L.; Loudes, C.; Blaise, A.; Klein, R.; Epelbaum, J.; Le Bouc, Y.; Holzenberger, M. Brain IGF-1 receptors control mammalian growth and lifespan through a neuroendocrine mechanism. *PLoS Biol.* **2008**, *6* (10), e254.

(20) Selman, C.; Lingard, S.; Choudhury, A. I.; Batterham, R. L.; Claret, M.; Clements, M.; Ramadani, F.; Okkenhaug, K.; Schuster, E.; Blanc, E.; Piper, M. D.; Al-Qassab, H.; Speakman, J. R.; Carmignac, D.; Robinson, I. C.; Thornton, J. M.; Gems, D.; Partridge, L.; Withers, D. J. Evidence for lifespan extension and delayed age-related biomarkers in insulin receptor substrate 1 null mice. *FASEB J.* **2008**, *22* (3), 807−18.
(21) Taguchi, A.; Wartschow, L. M.; White, M. F. Brain IRS2 signaling coordinates life span and nutrient homeostasis. *Science* **2007**, *317* (5836), 369−72.
(22) Selman, C.; Partridge, L.; Withers, D. J. Replication of extended lifespan phenotype in mice with deletion of insulin receptor substrate 1. *PLoS One* **2011**, *6* (1), e16144.
(23) Selman, C.; Tullet, J. M.; Wieser, D.; Irvine, E.; Lingard, S. J.; Choudhury, A. I.; Claret, M.; Al-Qassab, H.; Carmignac, D.; Ramadani, F.; Woods, A.; Robinson, I. C.; Schuster, E.; Batterham, R. L.; Kozma, S. C.; Thomas, G.; Carling, D.; Okkenhaug, K.; Thornton, J. M.; Partridge, L.; Gems, D.; Withers, D. J. Ribosomal protein S6 kinase 1 signaling regulates mammalian life span. *Science* **2009**, *326* (5949), 140−4.
(24) Harrison, D. E.; Strong, R.; Sharp, Z. D.; Nelson, J. F.; Astle, C. M.; Flurkey, K.; Nadon, N. L.; Wilkinson, J. E.; Frenkel, K.; Carter, C. S.; Pahor, M.; Javors, M. A.; Fernandez, E.; Miller, R. A. Rapamycin fed late in life extends lifespan in genetically heterogeneous mice. *Nature* **2009**, *460* (7253), 392−5.
(25) Miller, R. A.; Harrison, D. E.; Astle, C. M.; Baur, J. A.; Boyd, A. R.; de Cabo, R.; Fernandez, E.; Flurkey, K.; Javors, M. A.; Nelson, J. F.; Orihuela, C. J.; Pletcher, S.; Sharp, Z. D.; Sinclair, D.; Starnes, J. W.; Wilkinson, J. E.; Nadon, N. L.; Strong, R. Rapamycin, But Not Resveratrol or Simvastatin, Extends Life Span of Genetically Heterogeneous Mice. *J. Gerontol., A: Biol. Sci. Med. Sci.* **2011**, *66* (2), 191−201.
(26) Anisimov, V. N.; Berstein, L. M.; Egormin, P. A.; Piskunova, T. S.; Popovich, I. G.; Zabezhinski, M. A.; Tyndyk, M. L.; Yurova, M. V.; Kovalenko, I. G.; Poroshina, T. E.; Semenchenko, A. V. Metformin slows down aging and extends life span of female SHR mice. *Cell Cycle* **2008**, *7* (17), 2769−73.
(27) Anisimov, V. N.; Egormin, P. A.; Piskunova, T. S.; Popovich, I. G.; Tyndyk, M. L.; Yurova, M. N.; Zabezhinski, M. A.; Anikin, I. V.; Karkach, A. S.; Romanyukha, A. A. Metformin extends life span of HER-2/neu transgenic mice and in combination with melatonin inhibits growth of transplantable tumors in vivo. *Cell Cycle* **2010**, *9* (1), 188−97.
(28) McElwee, J. J.; Schuster, E.; Blanc, E.; Piper, M. D.; Thomas, J. H.; Patel, D. S.; Selman, C.; Withers, D. J.; Thornton, J. M.; Partridge, L.; Gems, D. Evolutionarily conservation of regulated longevity assurance mechanisms. *Genome Biol.* **2007**, *8* (7), R132.
(29) McCarroll, S. A.; Murphy, C. T.; Zou, S.; Pletcher, S. D.; Chin, C. S.; Jan, Y. N.; Kenyon, C.; Bargmann, C. I.; Li, H. Comparing genomic expression patterns across species identifies shared transcriptional profile in aging. *Nat. Genet.* **2004**, *36* (2), 197−204.
(30) Schumacher, B.; van der Pluijm, I.; Moorhouse, M. J.; Kosteas, T.; Robinson, A. R.; Suh, Y.; Breit, T. M.; van Steeg, H.; Niedernhofer, L. J.; van Ijcken, W.; Bartke, A.; Spindler, S. R.; Hoeijmakers, J. H.; van der Horst, G. T.; Garinis, G. A. Delayed and accelerated aging share common longevity assurance mechanisms. *PLoS Genet.* **2008**, *4* (8), e1000161.
(31) Miller, R. A.; Chang, Y.; Galecki, A. T.; Al-Regaiey, K.; Kopchick, J. J.; Bartke, A. Gene expression patterns in calorically restricted mice: partial overlap with long-lived mutant mice. *Mol. Endocrinol.* **2002**, *16* (11), 2657−66.
(32) Fuchs, S.; Bundy, J. G.; Davies, S. K.; Viney, J. M.; Swire, J. S.; Leroi, A. M. A metabolic signature of long life in Caenorhabditis elegans. *BMC Biol.* **2010**, *8*, 14.
(33) Nicholson, J. K.; Lindon, J. C.; Holmes, E. 'Metabonomics': understanding the metabolic responses of living systems to pathophysiological stimuli via multivariate statistical analysis of biological NMR spectroscopic data. *Xenobiotica* **1999**, *29* (11), 1181−9.
(34) Holmes, E.; Loo, R. L.; Stamler, J.; Bictash, M.; Yap, I. K.; Chan, Q.; Ebbels, T.; De Iorio, M.; Brown, I. J.; Veselkov, K. A.; Daviglus, M. L.; Kesteloot, H.; Ueshima, H.; Zhao, L.; Nicholson, J. K.; Elliott, P. Human metabolic phenotype diversity and its association with diet and blood pressure. *Nature* **2008**, *453* (7193), 396−400.
(35) Gavaghan, C. L.; Holmes, E.; Lenz, E.; Wilson, I. D.; Nicholson, J. K. An NMR-based metabonomic approach to investigate the biochemical consequences of genetic strain differences: application to the C57BL10J and Alpk:ApfCD mouse. *FEBS Lett.* **2000**, *484* (3), 169−74.
(36) Nicholson, J. K.; O'Flynn, M. P.; Sadler, P. J.; Macleod, A. F.; Juul, S. M.; Sonksen, P. H. Proton-nuclear-magnetic-resonance studies of serum, plasma and urine from fasting normal and diabetic subjects. *Biochem. J.* **1984**, *217* (2), 365−75.
(37) Nicholson, J. K.; Sadler, P. J.; Bales, J. R.; Juul, S. M.; MacLeod, A. F.; Sonksen, P. H. Monitoring metabolic disease by proton NMR of urine. *Lancet* **1984**, *2* (8405), 751−2.
(38) Wang, Z.; Klipfell, E.; Bennett, B. J.; Koeth, R.; Levison, B. S.; DuGar, B.; Feldstein, A. E.; Britt, E. B.; Fu, X.; Chung, Y.-M.; Wu, Y.; Schauer, P.; Smith, J. D.; Allayee, H.; Wilson Tang, W. H.; DiDonato, J. A.; Lusis, A. J.; Hazen, S. L. Gut flora metabolism of phosphatidylcholine promotes cardiovascular disease. *Nature* **2011**, *472*, 57−63.
(39) Mishur, R. J.; Rea, S. L. Applications of mass spectrometry to metabolomics and metabonomics: Detection of biomarkers of aging and of age-related diseases. *Mass Spectrom. Rev.* **2012**, *31* (1), 70−95.
(40) Yoshida, R.; Tamura, T.; Takaoka, C.; Harada, K.; Kobayashi, A.; Mukai, Y.; Fukusaki, E. Metabolomics-based systematic prediction of yeast lifespan and its application for semi-rational screening of ageing-related mutants. *Aging Cell* **2010**, *9* (4), 616−25.
(41) Martin, F. P.; Spanier, B.; Collino, S.; Montoliu, I.; Kolmeder, C.; Giesbertz, P.; Affolter, M.; Kussmann, M.; Daniel, H.; Kochhar, S.; Rezzi, S. Metabotyping of Caenorhabditis elegans and their culture media revealed unique metabolic phenotypes associated to amino acid deficiency and insulin-like signaling. *J. Proteome Res.* **2011**, *10* (3), 990−1003.
(42) Zhang, X.; Liu, H.; Wu, J.; Liu, M.; Wang, Y. Metabonomic alterations in hippocampus, temporal and prefrontal cortex with age in rats. *Neurochem. Int.* **2009**, *54* (8), 481−7.
(43) Nevedomskaya, E.; Meissner, A.; Goraler, S.; de Waard, M.; Ridwan, Y.; Zondag, G.; van der Pluijm, I.; Deelder, A. M.; Mayboroda, O. A. Metabolic profiling of accelerated aging ERCC1 d/- mice. *J. Proteome Res.* **2010**, *9* (7), 3680−7.
(44) Rezzi, S.; Martin, F. P.; Shanmuganayagam, D.; Colman, R. J.; Nicholson, J. K.; Weindruch, R. Metabolic shifts due to long-term caloric restriction revealed in nonhuman primates. *Exp. Gerontol.* **2009**, *44* (5), 356−62.
(45) Bartke, A.; Wright, J. C.; Mattison, J. A.; Ingram, D. K.; Miller, R. A.; Roth, G. S. Extending the lifespan of long-lived mice. *Nature* **2001**, *414* (6862), 412.
(46) Selman, C.; Kerrison, N. D.; Cooray, A.; Piper, M. D.; Lingard, S. J.; Barton, R. H.; Schuster, E. F.; Blanc, E.; Gems, D.; Nicholson, J. K.; Thornton, J. M.; Partridge, L.; Withers, D. J. Coordinated multitissue transcriptional and plasma metabonomic profiles following acute caloric restriction in mice. *Physiol. Genomics* **2006**, *27* (3), 187−200.
(47) Cao, S. X.; Dhahbi, J. M.; Mote, P. L.; Spindler, S. R. Genomic profiling of short- and long-term caloric restriction effects in the liver of aging mice. *Proc. Natl. Acad. Sci. U.S.A.* **2001**, *98* (19), 10630−5.
(48) Hempenstall, S.; Picchio, L.; Mitchell, S. E.; Speakman, J. R.; Selman, C. The impact of acute caloric restriction on the metabolic phenotype in male C57BL/6 and DBA/2 mice. *Mech. Ageing Dev.* **2010**, *131* (2), 111−8.
(49) Withers, D. J.; Gutierrez, J. S.; Towery, H.; Burks, D. J.; Ren, J. M.; Previs, S.; Zhang, Y.; Bernal, D.; Pons, S.; Shulman, G. I.; Bonner-Weir, S.; White, M. F. Disruption of IRS-2 causes type 2 diabetes in mice. *Nature* **1998**, *391* (6670), 900−4.
(50) Carr, H. Y.; Purcell, E. M. Effects of diffusion on free precession in nuclear magnetic resonance experiments. *Phys. Rev.* **1954**, *94*, 630−8.
(51) Meiboom, S.; Gill, D. Modified spin-echo method for measuring nuclear relaxation times. *Rev. Sci. Instrum.* **1958**, *29*, 688−91.

(52) Johnson, c. Diffusion ordered nuclear magnetic resonance spectroscopy: principles and applications. *Prog. Nucl. Magn. Reson. Spectrosc.* **1999**, *34*, 203−56.
(53) Liu, M.; Nicholson, J. K.; Lindon, J. C. High-resolution diffusion and relaxation edited one- and two-dimensional 1H NMR spectroscopy of biological fluids. *Anal. Chem.* **1996**, *68* (19), 3370−6.
(54) Veselkov, K. A.; Lindon, J. C.; Ebbels, T. M.; Crockford, D.; Volynkin, V. V.; Holmes, E.; Davies, D. B.; Nicholson, J. K. Recursive segment-wise peak alignment of biological (1)h NMR spectra for improved metabolic biomarker recovery. *Anal. Chem.* **2009**, *81* (1), 56−66.
(55) Dieterle, F.; Ross, A.; Schlotterbeck, G.; Senn, H. Probabilistic quotient normalization as robust method to account for dilution of complex biological mixtures. Application in 1H NMR metabonomics. *Anal. Chem.* **2006**, *78* (13), 4281−90.
(56) Wold, S.; Esbensen, K.; Geladi, P. Principle component analysis. *Chemom. Intell. Lab. Syst.* **1987**, *2*, 37−52.
(57) Trygg, J.; Wold, S. Orthogonal projections to latent structures (O-PLS). *J. Chemom.* **2002**, *16* (3), 119−28.
(58) Cloarec, O.; Dumas, M. E.; Trygg, J.; Craig, A.; Barton, R. H.; Lindon, J. C.; Nicholson, J. K.; Holmes, E. Evaluation of the orthogonal projection on latent structure model limitations caused by chemical shift variability and improved visualization of biomarker changes in H-1 NMR spectroscopic metabonomic studies. *Anal. Chem.* **2005**, *77* (2), 517−26.
(59) Neuhauser, M.; Manly, B. F. The Fisher-Pitman permutation test when testing for differences in mean and variance. *Psychol. Rep.* **2004**, *94* (1), 189−94.
(60) Nicholson, J. K.; Foxall, P. J. D.; Spraul, M.; Farrant, R. D.; Lindon, J. C. 750-MHz H-1 and H-1-C-13 Nmr-Spectroscopy of Human Blood-Plasma. *Anal. Chem.* **1995**, *67* (5), 793−811.
(61) Cloarec, O.; Dumas, M. E.; Craig, A.; Barton, R. H.; Trygg, J.; Hudson, J.; Blancher, C.; Gauguier, D.; Lindon, J. C.; Holmes, E.; Nicholson, J. Statistical total correlation spectroscopy: An exploratory approach for latent biomarker identification from metabolic H-1 NMR data sets. *Anal. Chem.* **2005**, *77* (5), 1282−9.
(62) Zahn, J. M.; Poosala, S.; Owen, A. B.; Ingram, D. K.; Lustig, A.; Carter, A.; Weeraratna, A. T.; Taub, D. D.; Gorospe, M.; Mazan-Mamczarz, K.; Lakatta, E. G.; Boheler, K. R.; Xu, X.; Mattson, M. P.; Falco, G.; Ko, M. S.; Schlessinger, D.; Firman, J.; Kummerfeld, S. K.; Wood, W. H. 3rd; Zonderman, A. B.; Kim, S. K.; Becker, K. G. AGEMAP: a gene expression database for aging in mice. *PLoS Genet.* **2007**, *3* (11), e201.
(63) Richards, S. E.; Wang, Y.; Lawler, D.; Kochhar, S.; Holmes, E.; Lindon, J. C.; Nicholson, J. K. Self-modeling curve resolution recovery of temporal metabolite signal modulation in NMR spectroscopic data sets: application to a life-long caloric restriction study in dogs. *Anal. Chem.* **2008**, *80* (13), 4876−85.
(64) Previs, S. F.; Withers, D. J.; Ren, J. M.; White, M. F.; Shulman, G. I. Contrasting effects of IRS-1 versus IRS-2 gene disruption on carbohydrate and lipid metabolism in vivo. *J. Biol. Chem.* **2000**, *275* (50), 38990−4.
(65) Araki, E.; Lipes, M. A.; Patti, M. E.; Bruning, J. C.; Haag, B. 3rd; Johnson, R. S.; Kahn, C. R. Alternative pathway of insulin signalling in mice with targeted disruption of the IRS-1 gene. *Nature* **1994**, *372* (6502), 186−90.
(66) Schirra, H. J.; Anderson, C. G.; Wilson, W. J.; Kerr, L.; Craik, D. J.; Waters, M. J.; Lichanska, A. M. Altered metabolism of growth hormone receptor mutant mice: a combined NMR metabonomics and microarray study. *PLoS One* **2008**, *3* (7), e2764.
(67) Ingram, D. K.; Roth, G. S. Glycolytic inhibition as a strategy for developing calorie restriction mimetics. *Exp. Gerontol.* **2011**, *46* (2−3), 148−54.
(68) Brown-Borg, H. M.; Johnson, W. T.; Rakoczy, S. G. Expression of oxidative phosphorylation components in mitochondria of long-living Ames dwarf mice. *Age (Dordr.)* **2012**, *34* (1), 43−57.
(69) Fenili, D.; Brown, M.; Rappaport, R.; McLaurin, J. Properties of scyllo-inositol as a therapeutic treatment of AD-like pathology. *J. Mol. Med.* **2007**, *85* (6), 603−11.
(70) Miller, R. A.; Buehner, G.; Chang, Y.; Harper, J. M.; Sigler, R.; Smith-Wheelock, M. Methionine-deficient diet extends mouse lifespan, slows immune and lens aging, alters glucose, T4, IGF-I and insulin levels, and increases hepatocyte MIF levels and stress resistance. *Aging Cell* **2005**, *4* (3), 119−25.
(71) Richie, J. P. Jr.; Leutzinger, Y.; Parthasarathy, S.; Malloy, V.; Orentreich, N.; Zimmerman, J. A. Methionine restriction increases blood glutathione and longevity in F344 rats. *FASEB J.* **1994**, *8* (15), 1302−7.
(72) Malloy, V. L.; Krajcik, R. A.; Bailey, S. J.; Hristopoulos, G.; Plummer, J. D.; Orentreich, N. Methionine restriction decreases visceral fat mass and preserves insulin action in aging male Fischer 344 rats independent of energy restriction. *Aging Cell* **2006**, *5* (4), 305−14.
(73) Uthus, E. O.; Brown-Borg, H. M. Altered methionine metabolism in long living Ames dwarf mice. *Exp. Gerontol.* **2003**, *38* (5), 491−8.
(74) Uthus, E. O.; Brown-Borg, H. M. Methionine flux to transsulfuration is enhanced in the long living Ames dwarf mouse. *Mech. Ageing Dev.* **2006**, *127* (5), 444−50.
(75) Speakman, J. R.; Selman, C. The free-radical damage theory: Accumulating evidence against a simple link of oxidative stress to ageing and lifespan. *Bioessays* **2011**, *33* (4), 255−9.
(76) Doonan, R.; McElwee, J. J.; Matthijssens, F.; Walker, G. A.; Houthoofd, K.; Back, P.; Matscheski, A.; Vanfleteren, J. R.; Gems, D. Against the oxidative damage theory of aging: superoxide dismutases protect against oxidative stress but have little or no effect on life span in Caenorhabditis elegans. *Genes Dev.* **2008**, *22* (23), 3236−41.
(77) Dominici, F. P.; Hauck, S.; Argentino, D. P.; Bartke, A.; Turyn, D. Increased insulin sensitivity and upregulation of insulin receptor, insulin receptor substrate (IRS)-1 and IRS-2 in liver of Ames dwarf mice. *J. Endocrinol.* **2002**, *173* (1), 81−94.
(78) Cruzen, C.; Colman, R. J. Effects of caloric restriction on cardiovascular aging in non-human priates and humans. *Clin. Geriatr. Med.* **2009**, *25* (4), 733−43; ix−x.
(79) Fontana, L.; Meyer, T. E.; Klein, S.; Holloszy, J. O. Long-term calorie restriction is highly effective in reducing the risk for atherosclerosis in humans. *Proc. Natl. Acad. Sci. U.S.A.* **2004**, *101* (17), 6659−63.
(80) Yap, I. K.; Brown, I. J.; Chan, Q.; Wijeyesekera, A.; Garcia-Perez, I.; Bictash, M.; Loo, R. L.; Chadeau-Hyam, M.; Ebbels, T.; De Iorio, M.; Maibaum, E.; Zhao, L.; Kesteloot, H.; Daviglus, M. L.; Stamler, J.; Nicholson, J. K.; Elliott, P.; Holmes, E. Metabolome-wide association study identifies multiple biomarkers that discriminate north and south Chinese populations at differing risks of cardiovascular disease: INTERMAP study. *J. Proteome Res.* **2010**, *9* (12), 6647−54.
(81) Rohwerder, T.; Breuer, U.; Benndorf, D.; Lechner, U.; Muller, R. H. The alkyl tert-butyl ether intermediate 2-hydroxyisobutyrate is degraded via a novel cobalamin-dependent mutase pathway. *Appl. Environ. Microbiol.* **2006**, *72* (6), 4128−35.
(82) Zeisel, S. H.; da Costa, K. A. Choline: an essential nutrient for public health. *Nutr. Rev.* **2009**, *67* (11), 615−23.
(83) Mehedint, M. G.; Niculescu, M. D.; Craciunescu, C. N.; Zeisel, S. H. Choline deficiency alters global histone methylation and epigenetic marking at the Re1 site of the calbindin 1 gene. *FASEB J.* **2010**, *24* (1), 184−95.
(84) Heiman, M. L.; Tinsley, F. C.; Mattison, J. A.; Hauck, S.; Bartke, A. Body composition of prolactin-, growth hormone, and thyrotropin-deficient Ames dwarf mice. *Endocrine* **2003**, *20* (1−2), 149−54.
(85) Haus, J. M.; Kashyap, S.; Kasumov, T.; Zhang, R.; DeFronzo, R.; Kirwan, J. P. Plasma Ceramide Subspecies are Elevated in Obese Subjects with Type 2 Diabetes and are Associated with the Level of Insulin Resistance. *Obesity* **2008**, *16*, S216.
(86) Jacobs, R. L.; Zhao, Y.; Koonen, D. P.; Sletten, T.; Su, B.; Lingrell, S.; Cao, G.; Peake, D. A.; Kuo, M. S.; Proctor, S. D.; Kennedy, B. P.; Dyck, J. R.; Vance, D. E. Impaired de novo choline synthesis explains why phosphatidylethanolamine N-methyltransferase-deficient mice are protected from diet-induced obesity. *J. Biol. Chem.* **2010**, *285* (29), 22403−13.

(87) Kinney, B. A.; Meliska, C. J.; Steger, R. W.; Bartke, A. Evidence that Ames dwarf mice age differently from their normal siblings in behavioral and learning and memory parameters. *Horm. Behav.* **2001**, *39* (4), 277−84.
(88) Sharma, S.; Haselton, J.; Rakoczy, S.; Branshaw, S.; Brown-Borg, H. M. Spatial memory is enhanced in long-living Ames dwarf mice and maintained following kainic acid induced neurodegeneration. *Mech. Ageing Dev.* **2010**, *131* (6), 422−35.
(89) Mattson, M. P. The impact of dietary energy intake on cognitive aging. *Front. Aging Neurosci.* **2010**, *2*, 5.
(90) Helms, S. A.; Azhar, G.; Zuo, C.; Theus, S. A.; Bartke, A.; Wei, J. Y. Smaller cardiac cell size and reduced extra-cellular collagen might be beneficial for hearts of Ames dwarf mice. *Int. J. Biol. Sci.* **2010**, *6* (5), 475−90.
(91) Dhahbi, J. M.; Tsuchiya, T.; Kim, H. J.; Mote, P. L.; Spindler, S. R. Gene expression and physiologic responses of the heart to the initiation and withdrawal of caloric restriction. *J. Gerontol., A: Biol. Sci. Med. Sci.* **2006**, *61* (3), 218−31.
(92) Guo, Z.; Mitchell-Raymundo, F.; Yang, H.; Ikeno, Y.; Nelson, J.; Diaz, V.; Richardson, A.; Reddick, R. Dietary restriction reduces atherosclerosis and oxidative stress in the aorta of apolipoprotein E-deficient mice. *Mech. Ageing Dev.* **2002**, *123* (8), 1121−31.
(93) Argentino, D. P.; Dominici, F. P.; Munoz, M. C.; Al-Regaiey, K.; Bartke, A.; Turyn, D. Effects of long-term caloric restriction on glucose homeostasis and on the first steps of the insulin signaling system in skeletal muscle of normal and Ames dwarf (Prop1df/Prop1df) mice. *Exp. Gerontol.* **2005**, *40* (1−2), 27−35.
(94) Brown-Borg, H. M.; Rakoczy, S. G.; Uthus, E. O. Growth hormone alters methionine and glutathione metabolism in Ames dwarf mice. *Mech. Ageing Dev.* **2005**, *126* (3), 389−98.
(95) Gabr, R. E.; El-Sharkawy, A. M.; Schar, M.; Weiss, R. G.; Bottomley, P. A. High-energy phosphate transfer in human muscle: the diffusion of phosphocreatine. *Am. J. Physiol. Cell Physiol.* **2011**, *301* (1), C234−41.
(96) Zhao, L. C.; Zhang, X. D.; Liao, S. X.; Gao, H. C.; Wang, H. Y.; Lin, D. H. A metabonomic comparison of urinary changes in Zucker and GK rats. *J. Biomed. Biotechnol.* **2010**, *2010*, 431894.
(97) Biagi, E.; Nylund, L.; Candela, M.; Ostan, R.; Bucci, L.; Pini, E.; Nikkila, J.; Monti, D.; Satokari, R.; Franceschi, C.; Brigidi, P.; De Vos, W. Through ageing, and beyond: gut microbiota and inflammatory status in seniors and centenarians. *PLoS One* **2010**, *5* (5), e10667.
(98) Woodmansey, E. J. Intestinal bacteria and ageing. *J. Appl. Microbiol.* **2007**, *102* (5), 1178−86.